Asian Journal of Chemistry; Vol. 26, No. 8 (2014), 2403-2406

ASIAN JOURNAL OF CHEMISTRY

http://dx.doi.org/10.14233/ajchem.2014.16031

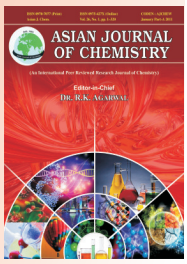

H_2 Plasma Treatment to Prepare Reduced TiO_2 Catalyst with High Oxygen Vacancies Content

S.Z. HU[1,*], Z.L. KANG[2], Z.W. NING[2], J.H. YE[2], F.Y. LI[1] and Z.P. FAN[1]

[1]Institute of Eco-environmental Sciences, Liaoning Shihua University, Fushun 113001, P.R. China
[2]School of Petrochemical Engineering, Liaoning Shihua University, Fushun 113001, P.R. China

*Corresponding author: Tel: +86 24 23847473; E-mail: hushaozheng001@163.com

Received: 11 July 2013; *Accepted*: 21 August 2013; *Published online*: 15 April 2014; AJC-15035

A visible light responsive TiO_2 with high oxygen vacancies content were prepared *via* H_2 plasma treatment. X-ray diffraction, UV-visible spectroscopy, Raman and X-ray photoelectron spectroscopy were used to characterize the prepared TiO_2 samples. The plasma treatment extended its absorption edges to the visible light region. Large amount of oxygen vacancies were created which proved by XRD and Raman. The photocatalytic activities were tested in the degradation of an aqueous solution of a reactive dyestuff, methylene blue, under visible light. The photocatalytic activities of TiO_2 was influenced by the oxygen vacancies content. A possible mechanism for the photocatalysis was proposed.

Keywords: Oxygen vacancies, Ti^{3+} species, TiO_2, Methylene blue, Photocatalysis.

INTRODUCTION

Semiconductor materials have attracted more and more attention as photocatalytic materials. Titanium dioxide is the most promising one of the semiconductor photocatalysts because of its nontoxicity, long-term stability and low cost[1]. Titanium dioxide is widely used in various fields, such as removal of organic and inorganic pollutants[2-4], dye-sensitized solar cells, photocatalytic splitting of water for green-energy hydrogen production and so on[5]. However, TiO_2 can only absorb ultraviolet light due to its wide band-gap energy (3.0-3.2 eV), leading to absorption in only a small region of the solar spectrum. Moreover, the undesired recombination of photoexcited carriers limited the effective application of TiO_2 seriously[6]. Recently, to improve the photocatalytic activity of TiO_2 and extend its light absorption region several approaches have been proposed, such as, non-metal-doping[7], shaped-control[8,9], and surface-modifying[10,11].

Among those dopant, nitrogen was considered as the most promising one. In 1986, Sato reported for the first time that N-doped TiO_2 obtained by annealing $Ti(OH)_4$ mixed with NH_4Cl or NH_4OH showed visible light activity[12]. He ascribed the visible light sensitization to NOx impurities in the TiO_2 lattice. Since then, N-doping has become a hot topic and been widely investigated. However, up to date, the mechanism of the enhancement by N-doping is still controversial. Asahi *et al.*[13] prepared nitrogen doped TiO_2 films by sputtering TiO_2 in a N_2/Ar gas mixture in 2001 and concluded that the doped N atoms narrowed the band gap of TiO_2 by mixing N 2p and O 2p states, therefore demonstrating the activity for the decomposition of acetone and methylene blue. Irie *et al.*[14] argued that the isolated narrow band located above the valence band is responsible for the visible light response. Ihara *et al.*[15] suggested that the visible light activity is attributed to the oxygen vacancies which caused by N-doping.

Non-thermal plasma is composed of atoms, ions and electrons, which are much more reactive than their molecule precursors. Plasma is able to initiate a lot of reactions, which take place efficiently only at elevated temperatures and high pressures, under mild conditions. So far, some literatures on preparation of TiO_2 by plasma treatment have been reported. However, the effect of oxygen vacancies produced by plasma treatment on the photocatalytic performance of TiO_2 is unclear. In this work, reduced TiO_2 was prepared by H_2 plasma treatment. The photocatalytic performances of prepared samples were evaluated in the degradation of methylene blue under visible light. The possible mechanism was presented.

EXPERIMENTAL

Reduced TiO_2 was conducted in a dielectric barrier discharge (DBD) reactor, consisting of a quartz tube and two electrodes. The high-voltage electrode was a stainless-steel rod (2.5 mm), which was installed in the axis of the quartz tube and connected to a high voltage supply. The grounding electrode was an aluminum foil which was wrapped around the quartz tube. For each run, 0.4 g commercial TiO_2 powder

(P25) was charged into the quartz tube. H_2 from a gas cylinder was allowed to pass through the bed for 3 min to flush out the air. At a constant H_2 flow (80 mL min^{-1}), a high voltage of 9-11 kV was supplied by a plasma generator at an overall power input of 50 V × 0.4 A. The discharge frequency was fixed at 10 kHz and the discharge was kept for 3-30 min. The obtained TiO_2 sample was denoted as RT-x, in which, x stands for the H_2-plasma discharge time (min).

X-ray diffraction (XRD) patterns of the prepared TiO_2 samples were recorded on a Rigaku D/max-2400 instrument using Cu-K_α radiation (λ = 1.54 Å). UV-visible spectroscopy measurement was carried out on a Jasco V-550 spectrophotometer, using $BaSO_4$ as the reference sample. XPS measurements were conducted on a Thermo Escalab 250 XPS system with Al K_α radiation as the exciting source. The binding energies were calibrated by referencing the C 1s peak (284.6 eV) to reduce the sample charge effect.

Methylene blue was selected as model compound to evaluate the photocatalytic performance of the prepared TiO_2 particles in an aqueous solution under visible light irradiation. Titanium dioxide powder (0.1 g) were dispersed in 100 mL aqueous solution of methylene blue (50 ppm) in an ultrasound generator for 10 min. The suspension was transferred into a self-designed glass reactor and stirred for 0.5 h in darkness to achieve the adsorption equilibrium. In the photoreaction under visible light irradiation, the suspension was exposed to a 110-W high-pressure sodium lamp with main emission in the range of 400-800 nm and air was bubbled at 130 mL/min through the solution. The UV light portion of sodium lamp was filtered by 0.5 M $NaNO_2$ solution. All runs were conducted at ambient pressure and 30 °C. At given time intervals, 4 mL suspension was taken and immediately centrifuged to separate the liquid samples from the solid catalyst. The concentrations of methylene blue before and after reaction were measured by means of a UV-visible spectrophotometer at a wavelength of 665 nm. It is the linear relationship between absorbance and concentration of liquid sample in the experimental concentration range. Therefore, the percentage of degradation D % was determined by the absorbances of the liquid sample before and after degradation.

RESULTS AND DISCUSSION

The XRD patterns of P25, RT-3, RT-8, RT-15, RT-20, RT-30 are shown in Fig. 1. All the samples were the mixture of anatase and rutile phase. There was no observable structural difference between neat and modified TiO_2 samples. The lattice parameters of the catalysts were measured using (1 0 1) and (2 0 0) in anatase crystal planes by using equations:

$$d_{(hkl)} = \frac{\lambda}{2\sin\theta} \quad (1)$$

$$d_{(hkl)}^{-2} = h^2a^{-2} + k^2b^{-2} + l^2c^{-2} \quad (2)$$

where $d_{(h\,k\,l)}$ is the distance between crystal planes of (h k l), λ is the X-ray wavelength, θ is the diffraction angle of crystal plane (h k l), h k l is the crystal index. The a, b and c are lattice parameters (in anatase form, a = b ≠ c). The results shown in Table-1 indicated that the lattice parameters of all samples remain almost unchanged along a- and b-axes, whereas the c-axis parameter decreased for H_2 plasma treated samples. This indicated that TiO_2 was reduce and oxygen vacancies were formed, leading to the decrease in the cell volume. In Fig. 2, the peak is fitted with a pseudo-Voigt function and plotted as a function of the oxygen vacancies contnt (obtained from XPS data). After plasma treatment, the anatase (101) peak position shifts toward smaller d values with increasing oxygen vacancies concentration. The observed shift is linear with the amount of plasma treated time, which proves that the oxygen vacancies were formed by H_2 plasma treatment.

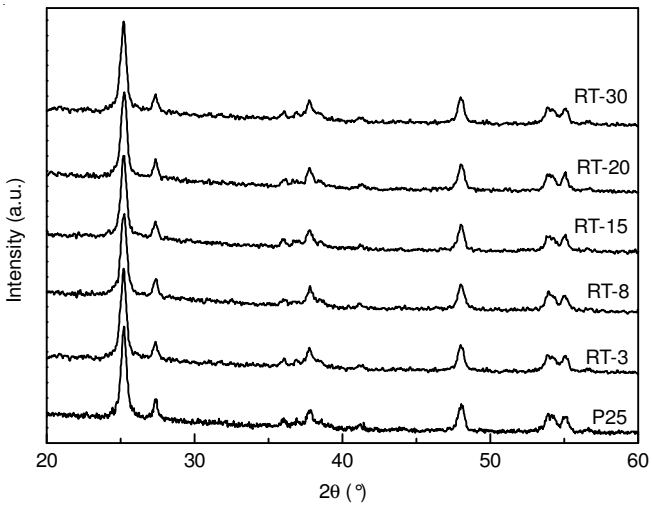

Fig. 1. XRD patterns of P25 and reduced TiO_2 samples

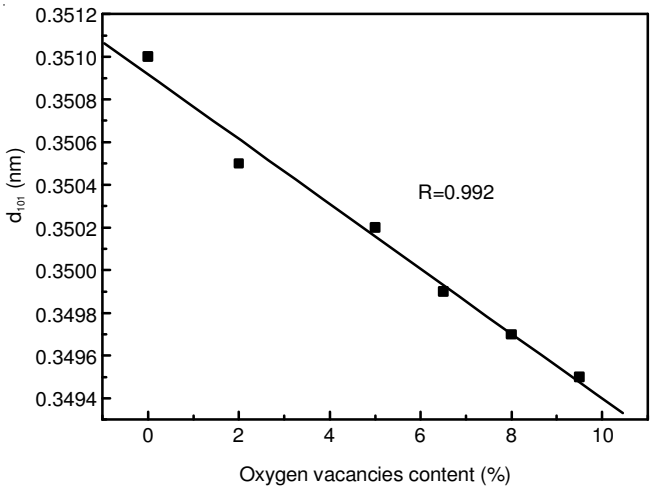

Fig. 2. Relationship of d_{101} lattice spacing and oxygen vacancies contents

Fig. 3 showed the UV-visible diffuse reflectance spectra of P25 and reduced TiO_2 nanoparticles. No obvious shifts of the absorption bands into the visible light region were observed for reduced TiO_2 catalysts. In the spectrum of RT-15, the obvious absorption in 400-520 nm is observed, which should be attributed the formation of oxygen vacancies. DFT calculations suggested that energy level of oxygen vacancies was about 0.8 eV below the bottom of the conduction band[16,17]. According to the method of Oregan and Gratzel[18], the binding energy of RT-15 is 2.38 eV, which is exactly 0.8 eV lower than that of pure TiO_2. Thus, this visible light adsorption should be due to the presence of oxygen vacancies in the sample.

XPS is an effective surface test technique for characterizing elemental composition and chemical states. The XPS data

TABLE-1
XPS DATA OF P25 AND H_2 PLASMA TREATED CATALYSTS

Catalyst	O atom		Ti atom		O/Ti
	Binding energy (eV)	atm. (%)	Binding energy (eV)	atm. (%)	
P25	530.5	66.6	458.4	33.4	2.0
RT-3	530.5	66.2	458.4	33.8	1.96
RT-8	530.4	65.5	458.2	34.5	1.9
RT-15	530.2	65.1	458.0	34.9	1.87
RT-20	530.0	64.8	457.9	35.2	1.84
RT-30	530.0	64.4	457.8	35.6	1.81

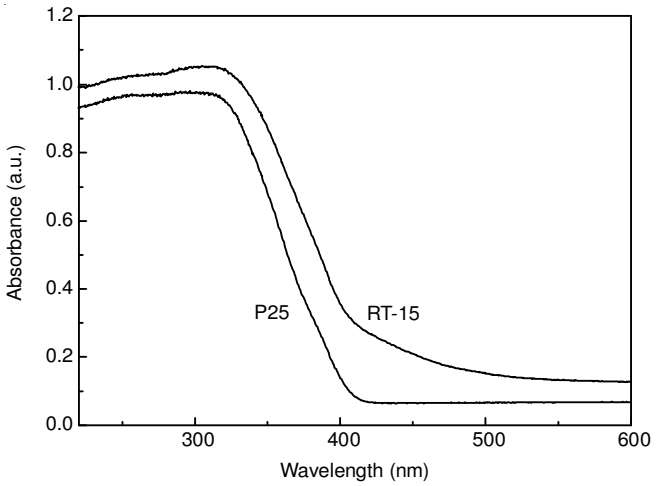

Fig. 3. UV-visible diffuse reflectance spectra of P25 and RT-15

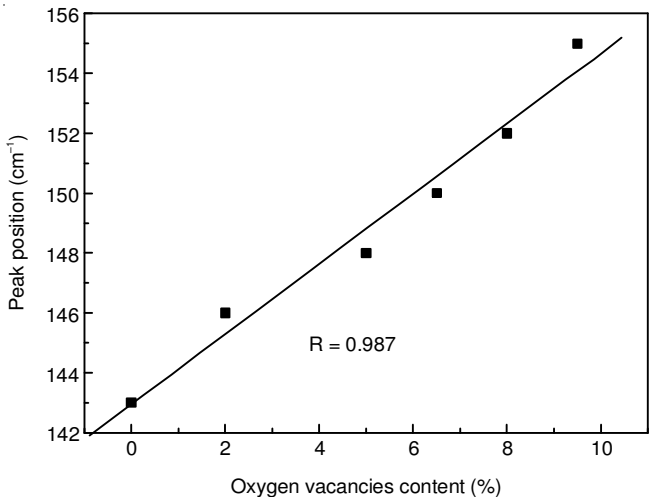

Fig. 4. Relationship of peak positions of the strongest anatase E_g vibrational mode and oxygen vacancies contents

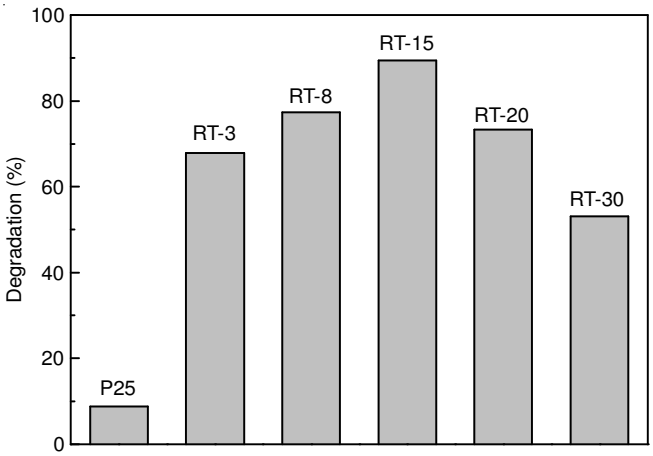

Fig. 5. Photocatalytic performances of P25 and plasma treated TiO_2 catalysts in the degradation methylene blue (reaction time: 6h)

were shown in Table-1. The binding energy of Ti 2p and O1s for P25 were 530.5 and 458.4 eV. After plasma treatment, the binding energies shift to lower value with increasing the plasma treated time. This is due to the formation of Ti ions with low valence by H_2 plasma reduction, which is consistent with previous reports. Besides, the O/Ti ratio for P25 was 2.0, whereas this value was decreased obviously with increasing the plasma treated time. After 0.5 h H_2 plasma reduction, the O/Ti ratio was only 1.81, indicating large amount of oxygen vacancies were formed by this reduction process.

The anatase phase shows major Raman bands at 144, 197, 399, 515, 519 and 639 cm^{-1} whereas the typical Raman bands related to the rutile phase appear at 143, 235, 447 and 612 cm^{-1}. Raman spectrum of P25 and reduced TiO_2 catalysts (not shown here) indicates that all the samples are the mixture of anatase and rutile phase, which is consistent with XRD result. Besides, it is shown that, with the increasing of plasma treated time, the peak position of E_g vibrational mode shift to the lower wavenumber. Fig. 4 shows the relationship of peak positions of the strongest anatase E_g vibrational mode and oxygen vacancies contents. Obviously, a well linear relationship was obtained (R = 0.987).

Fig. 5 showed the results of the photocatalytic performance of reduced TiO_2 samples in the degradation methylene blue under visible light. For P25, the activity was poor. However, after H_2 plasma treatment, the photocatalytic activities of obtained catalysts were obviously improved. RT-15 exhibited the highest photocatalytic activity, about 90 % of methylene blue degreade after 6 h. This is probably due to the formation of oxygen vacancies by the H_2 plasma reduction. DFT calculations suggested that energy level of oxygen vacancies was was about 0.8 eV below the bottom of the conduction band. Thus the TiO_2 could absorb the visible light and excited the electrons to the energy level of oxygen vacancies, then to the conduction band and form the active oxygen species. Besides, it is shown that the activity of H_2 reduced TiO_2 catalysts increased firstly from RT-3 to RT-15. With further increase the plasma treated time, the activity decreased obviously. This is probably due to the difference of oxygen vacancies content among the prepared samples. With low oxygen vacancies content, it can trap the photogenerated electrons, thus not only improve the absorption of visible light but also restrain the recombination of electrons and holes. However, with the excess oxygen

vacancies content, the energy level of oxygen vacancies will become the recombination center of photogenerated electrons and holes, although the absorption of visible light was further increased. Thus the optimal oxygen vacancies content was obtained in RT-15, which showed the highest photocatalytic activity.

Conclusion

H_2 plasma reduced TiO_2 nanoparticles was prepared. UV-visible diffuse reflectance spectra showed that reduced TiO_2 exhibited obvious absorption in the visible light range, which was ascribed to the presence of oxygen vacancy state between the valence and the conduction bands. The oxygen vacancies content increased with increasing the plasma treated time. The photocatalytic activity of prepared catalyst increased firstly and then decreased with further increase the plasma treated time, because the excess oxygen vacancies content act as the recombination center. The optimal oxygen vacancies content was obtained for RT-15, which showed the highest activity *i.e.*, 90 % degradation of methylene blue after 6 h.

ACKNOWLEDGEMENTS

This work was supported by National Natural Science Foundation of China (No. 41071317, 30972418), National Key Technology R & D Programme of China (No. 2007BA C16B07, 2012ZX07505-001), the Natural Science Foundation of Liaoning Province (No. 20092080).

REFERENCES

1. K. Yang, Y. Dai and B. Huang, *Phys. Rev. B*, **76**, 195201 (2007).
2. N. Bahadur, K. Jain, A.K. Srivastava, Govind, R. Gakhar, D. Haranath and M.S. Dulat, *Mater. Chem. Phys*., **124**, 600 (2010).
3. A. Folli, S.B. Campbell, J.A. Anderson and D.E. Macphee, *J. Photochem. Photobiol. A*, **220**, 85 (2011).
4. M.C. Sansiviero, D.S. dos Santos, A.E. Job and R.F. Aroca, *J. Photochem. Photobiol. A*, **220**, 20 (2011).
5. M.R. Hoffmann, S.T. Martin, W.Y. Choi and D.W. Bahnemann, *Chem. Rev*., **95**, 69 (1995).
6. D.M. Chen, D. Yang, Q. Wang and Z. Jiang, *Ind. Eng. Chem. Res*., **45**, 4110 (2006).
7. Y. Yalcin, M. Kilic and Z. Cinar, *J. Adv. Oxid. Technol*., **13**, 281 (2010).
8. T. Sugimoto, X.P. Zhou and A. Muramatsu, *J. Colloid Interf. Sci*., **259**, 53 (2003).
9. S. Chu, L.L. Luo, J.C. Yang, F. Kong, S. Luo, Y. Wang and Z.G. Zou, *Appl. Surf. Sci*., **258**, 9664 (2012).
10. T. Arita, K. Moriya, T. Yoshimura, K. Minami, T. Naka and T. Adschiri, *Ind. Eng. Chem. Res*., **49**, 9815 (2010).
11. M.L. Luo, J.Q. Zhao, W. Tang and C.S. Pu, *Appl. Surf. Sci*., **249**, 1 (2005).
12. S. Sato, *Chem. Phys. Lett*., **123**, 126 (1986).
13. R. Asahi, T. Morikawa, T. Ohwaki, A. Aoki and Y. Taga, *Science,* **293**, 269 (2001).
14. H. Irie, Y. Watanabe and K. Hashimoto, *J. Phys. Chem. B*, **107**, 5483 (2003).
15. T. Ihara, M. Miyoshi, Y. Iriyama, O. Matsumoto and S. Sugihara, *Appl. Catal. B*, **42**, 403 (2003).
16. M.A. Henderson, W.S. Epling, C.H.F. Peden and C.L. Perkins, *J. Phys. Chem. B*, **107**, 534 (2003).
17. S. Livraghi, M.C. Paganini, E. Giamello, A. Selloni, C. Di Valentin and G. Pacchioni, *J. Am. Chem. Soc*., **128**, 15666 (2007).
18. B. Oregan and M. Gratzel, *Nature*, **353**, 737 (1991).